



ELSEVIER

Optics and Lasers in Engineering 37 (2002) 187–202

---

---

OPTICS and LASERS  
in  
ENGINEERING

---

---

# Emission Fourier transform spectroscopy for the remote sensing of the atmosphere

Giovanni Bianchini\*, Ugo Cortesi, Luca Palchetti

*Istituto di Ricerca sulle Onde Elettromagnetiche “Nello Carrara”, Via Panciatichi 64, 50127 Firenze, Italy*

Received 30 April 2001; accepted 19 June 2001

---

## Abstract

Fourier transform spectrometers (FTS), thanks to their intrinsic advantages of high throughput, high spectral resolution and multiplex acquisition of spectral channels, offer a powerful tool for the characterisation of the Earth's atmosphere. The use of photon noise limited detectors in FTS instruments operating in the middle/far infrared spectral region permits high sensitivity emission spectroscopy measurements, without the limitations arising from the use of an external radiation source. The wide operating spectral range of FTS instruments makes possible simultaneous detection of different atmospheric chemical species that show rotational and vibrational spectral bands in the middle/far infrared region.

Spatially resolved measurements of the concentration of the interesting species are of fundamental interest in the study of local phenomena in atmospheric chemistry and physics, and can be obtained through the use of various observation and data inversion techniques. Among these, the best results in terms of vertical resolution are achieved through the limb sounding observation technique from airborne platform.

As an example of possibilities offered by the above considered technique, results obtained from the SAFIRE-A (Spectroscopy of the Atmosphere using Far InfraRed Emission-Airborne) during the Antarctic campaign APE-GAIA (Airborne Polar Experiment-Geophysica Aircraft In Antarctica, Ushuaia, Argentina, September–October, 1999) are presented. © 2002 Elsevier Science Ltd. All rights reserved.

*Keywords:* Fourier transform spectroscopy; Emission spectroscopy; Earth observation; Stratospheric chemistry

---

---

\*Corresponding author.

*E-mail address:* gb@iroe.fi.cnr.it (G. Bianchini).

## 1. Emission spectroscopy of the atmosphere

A number of chemical, dynamical and radiative processes, affecting the physical structure and the composition of the Earth's atmosphere, can be investigated by measuring spontaneous thermal emission of atmospheric molecules. Emission spectroscopy benefits by unique advantages in comparison with other remote sensing methods [1,2]. Being a passive technique, it does not introduce perturbations in the observed air masses and does not require energy demanding instruments. Moreover, emission measurements provide a better geographical and temporal coverage compared to absorption measurements. They do not need an external radiation source and can be performed continuously (both at day and at night) in all the directions. This allows to overcome the poor latitude coverage of occultation measurements and makes possible to monitor several key processes that involve chemical species with a diurnal cycle. On the other hand, observations of the signal emitted by atmospheric molecules are only possible within the frequency range with significant thermal emission from the atmosphere; this includes the middle/far IR and the millimetre spectral regions and its boundaries are defined by a low frequency cut-off (approximately  $3\text{ cm}^{-1}$ ) caused by the limits of optical instruments (to which instruments this discussion is confined) and by a high frequency cut-off (approximately  $3000\text{ cm}^{-1}$ ) due to the low number of emitted photons.

### 1.1. The atmospheric emission spectrum

The emission spectrum of the Earth's atmosphere consists of spectral features that correspond to rotational and vibrational transitions of the atmospheric molecules (main gases and minor constituents). Pure rotational bands are associated to the millimetre ( $3\text{--}30\text{ cm}^{-1}$ ) and the far infrared (FIR,  $30\text{--}300\text{ cm}^{-1}$ ) part of the spectrum, vibration bands to the middle infrared region (MIR,  $300\text{--}3000\text{ cm}^{-1}$ ). The intensity envelope is given by the spectral distribution of a blackbody at the temperature of the emitting air masses (typically  $250\text{ K}$  in the stratosphere). The dependence of the Planck function on temperature, for small variations around a fixed value  $T_0$ , can be expressed as:

$$B(\sigma, T) = c(\sigma) \left( \frac{T}{T_0} \right)^{n(\sigma)},$$

where the term  $c(\sigma)$  does not depend on the temperature and the exponent  $n(\sigma)$  is approximately 1 at low frequencies (for instance,  $\sigma \ll 170\text{ cm}^{-1}$  around  $T_0 = 250\text{ K}$ ) and rapidly increases as the frequency is increased. The emission in the MIR is, therefore, very sensitive to atmospheric temperature. Temperature profiles can be retrieved with high accuracy by measuring the emission spectrum of a species with well know volume mixing ratio distribution. Conversely, a very good knowledge of the temperature profile is required for retrieving minor constituents concentration from emission measurements in the MIR. From this perspective, measurements in the FIR are relatively easier and can take advantage also from further aspects such as the freedom from scattering due to aerosols and clouds particles.

The complementarity of emission measurements in the MIR and FIR region can be recognised also in the coverage of the chemical species. Apart from some main gases (for instance, water vapour and ozone), that have ubiquitous spectra in the infrared region, in the middle infrared it is possible to measure almost the entire nitrogen family, including the source gas  $\text{N}_2\text{O}$  and the important reservoir species  $\text{ClONO}_2$  with the only exception of  $\text{NO}_3$ . The detection of several compounds, that cannot be measured in the FIR, is also relatively easy in the MIR: for instance  $\text{CO}_2$  and  $\text{CH}_4$  (which, having a dipole moment equal to zero, do not display a pure rotational spectrum) or the chlorofluorocarbons. FIR remote sounders have their strength in the observation of hydrogen family. ( $\text{OH}$ ,  $\text{HO}_2$ ,  $\text{H}_2\text{O}_2$ ), but can also measure chlorine species ( $\text{HCl}$ ,  $\text{HOCl}$  and  $\text{ClO}$ ), bromine species ( $\text{HBr}$ ,  $\text{HOBr}$  and  $\text{BrO}$ ) and, even if with less sensitivity compared to the MIR, a few compounds of the nitrogen family ( $\text{N}_2\text{O}$ ,  $\text{HNO}_3$ ).

### 1.2. Observing geometries and techniques

Different combinations of the observation platform (ground-based stations, high altitude platforms or satellites) and of the viewing geometry (vertical sounding or limb sounding) can be chosen, in principle, for remote-sensing of the Earth's atmosphere. Vertical sounding can be performed either from the ground, looking at the zenith, or from high altitude and space-borne platforms in nadir looking mode. Limb sounding measurements are possible from stratospheric balloon and aircraft, as well as from space. Each of these options offers specific advantages and disadvantages, with limb sounding being particularly well suited for the study of upper tropospheric and lower stratospheric chemistry.

Despite their wider spatial and temporal coverage, limb sounding observations from space have limited capability of capturing small scale features in the lowest altitude range. In fact, balloon and airborne instruments are usually the best choice for detailed investigations of the physical and chemical structure of the upper troposphere and lowermost stratosphere and for the study of local phenomena. The operating altitude of large stratospheric balloons (approximately 40 km) is higher than the ceiling of highflying aircraft (20 km) and offer a better chance for limb scanning. On the other hand, the mobility and manoeuvrability of the aircraft, as well as the possibility of performing several flights within a relatively short time period cannot be obtained with balloon-borne instrumentation. Moreover, large scientific payload can be accommodated aboard an aircraft, making possible simultaneous measurements of several chemical compounds and other atmospheric parameters.

### 1.3. Limb sounding observation scheme

The concept of limb sounding observation geometry is illustrated in Fig. 1a the instrument aboard a high altitude platform or satellite observes radiation emitted or absorbed by the air masses along a line of sight tangent to an atmospheric layer. The main contribution to the observed signal, as shown in the figure, comes from

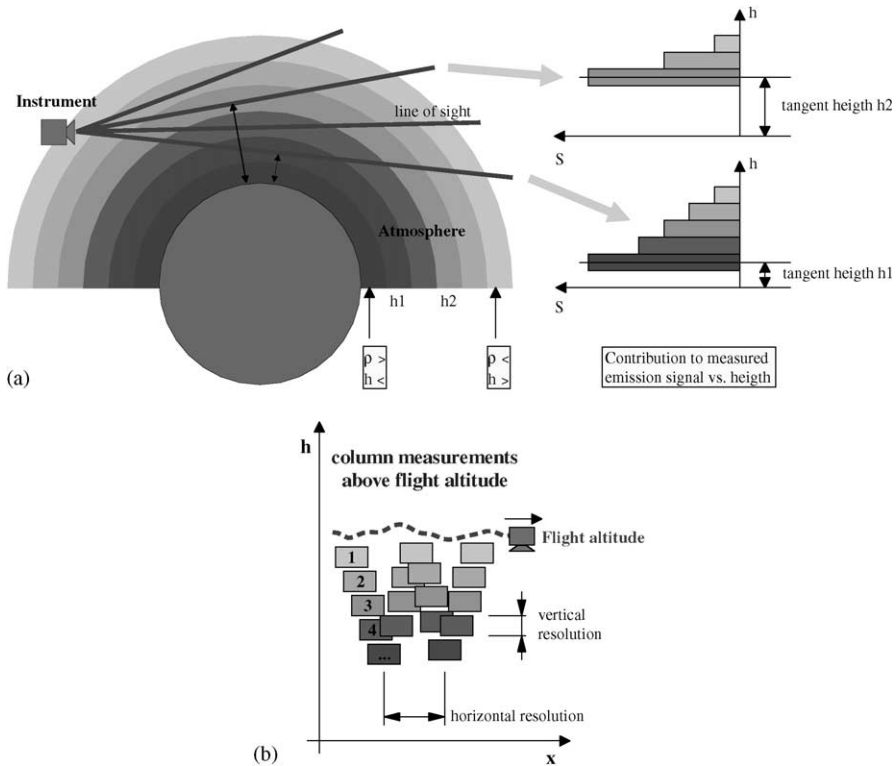


Fig. 1. Scheme of the limb-sounding observation geometry. (a) response of a limb-sounding emission spectrometer to contribution of different atmospheric layers. (b) spatial coverage of measurements from a limb-sounding instrument operating on an atmospheric platform.

the lowest atmospheric layer intersected by the line of sight, thus making limb sounding measurements highly selective in the vertical direction.

The main advantages of limb geometry compared to the vertical sounding are:

1. the absorbing (or emitting) path is larger and delivers detectable signals also from very weak absorbers (or emitters),
2. emission measurements are made with deep space, rather than warm Earth's surface, at the end of the line of sight,
3. high vertical resolution is obtained, typically of 2–3 km, with the possibility of scanning the line of sight across the atmospheric layers and retrieving the vertical concentration profiles from a sequence of measurements performed at different limb angles.

A drawback of a limb sounding measurement is the poor horizontal resolution in the direction perpendicular to the aircraft heading, typically about 500 km, due to the very long distances travelled by the line of sight in the atmosphere. The

resolution along the flight path, as shown in Fig. 1b, is instead given by the product of limb scanning sequence acquisition time and aircraft ground speed.

#### 1.4. Fourier transform spectroscopy for earth observation

A wealth of spectroscopic techniques and instruments is available nowadays for passive emission sounding of the Earth's atmosphere. Among these, Fourier transform spectroscopy (FTS) still represents the preferred option in several studies, whose measurement requirements are only partially satisfied by competing techniques. In fact, Fourier transform spectrometers provide a specific combination of attributes that can efficiently match different observing needs, such as those imposed, for instance, by investigation of upper tropospheric and lower stratospheric chemistry. The classical advantages of FTS can be fully exploited when applied to atmospheric measurements: the detection of very weak signals emitted (or absorbed) by atmospheric molecules and their acquisition with adequate temporal and spatial resolution become possible only because of the gain introduced by the *throughput* and the *multiplex advantage* [3]. Furthermore, the capability of resolving spectral features due to minor middle atmospheric constituents is granted by the high spectral resolution provided by FTS measurements, which can easily meet the typical requirement for a resolving power better than 10,000 (corresponding to a limit spectral resolution of  $0.1 \text{ cm}^{-1}$  in the MIR and of  $0.01 \text{ cm}^{-1}$  in the FIR). This results in a fundamental advantage when coupled with the broadband operation potential of Fourier transform instruments, that permits the simultaneous measurement of a large suite of chemical compounds.

## 2. The SAFIRE-A FTS spectrometer

SAFIRE-A is a particular implementation of the Martin–Puplett [4] polarising FT spectrometer specially designed for airborne operation [5]. The principal instrumental characteristics are summarised in Table 1. Optical path folding and a misalignment-compensating [6] optical scheme have permitted to enclose the whole instrument, including optics, control and data storage electronics and cryogenic detectors in a compact package suitable for integration on the Russian M-55 Geophysica high altitude aircraft (Fig. 2).

The M-55 Geophysica, a modified version of a former reconnaissance aircraft operated by the Myasishchev Design Bureau, is together with the American ER-2 the only platform available in the world for stratospheric research. It is a dual turbofan single-seater aircraft capable of flying, both at day and at night, in all weather conditions. The platform can operate at a ceiling altitude of 21 km for about 5 h. The maximum cruise ground speed is about  $750 \text{ km h}^{-1}$  and the operative radius at 17 km altitude is approximately 3500 km. The M-55 Geophysica has unique capabilities for carrying large scientific instruments: it can accommodate a payload with a weight up to a maximum of 1500 kg and with a total volume of up to  $12 \text{ m}^3$ . A large reserve of

Table 1  
SAFIRE-A instrumental specifications

Parameter	Value
Instrument type	Polarising FT spectrometer
Dimensions	1800 × 880 × 650 mm <sup>3</sup>
Weight	387 kg
Interferogram acquisition time	12, 24, 48, 96 s
Number of detection channels	2
Operating spectral range	10–250 cm <sup>-1</sup>
Maximum spectral resolution	0.004 cm <sup>-1</sup>
Vertical resolution	About 1.5 km
Vertical field of view	0.57°
Spectral signal-to-noise ratio	> 500
Observation technique	Limb-sounding emission



Fig. 2. The M-55 Geophysica aircraft.

electric power (60 kW at 115 VAC and 3 kW at 27.5 VDC) makes it possible to embark also energy demanding instruments (e.g. high power lidars).

### 2.1. Instrument optical layout

As shown in Fig. 3, the SAFIRE-A instrument is made of three main parts, the input optics system, the interferometer, and the cold optics and detector module

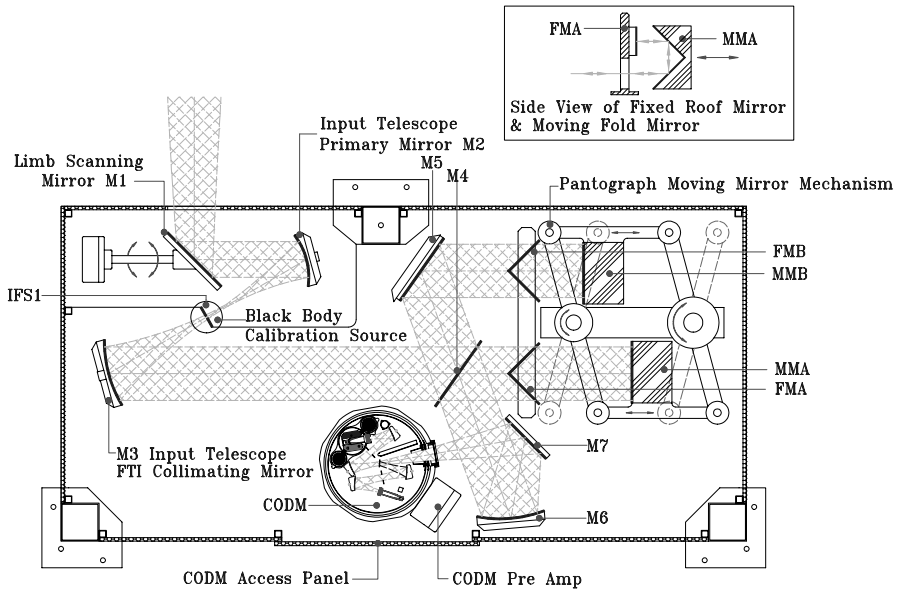


Fig. 3. Scheme of the SAFIRE-A instrument layout.

(CODM) including output optics and detectors. Atmospheric emission is collected through a pointing mirror which is controlled in position using the roll angle information provided by the aircraft navigation system with an accuracy of about 20 arcsec. A calibration system, located in the focus of the input telescope, permits to choose the reference source from two calibration blackbodies at different temperatures.

The FIR interferometer is based on a double parallelogram scheme that through a folding of the optical path and the simultaneous movement of both mirrors provide a maximum optical path difference (OPD) between the two arms of the interferometer equal to 1.25 m, containing the optics in a cube with a side of about 0.5 m. Accurate measurement of OPD is obtained through a reference laser interferometer based on a frequency-stabilised diode laser source and following the same optical path of the far infrared radiation [7].

The CODM encloses output optics, including pupils and field stops, blocking filters and collecting optics, and the two detectors corresponding to the two acquisition channels. All these components are mounted on the cold plate of a liquid helium cryostat, and allow the full exploitation of photon-noise limited detectors. Two different kinds of infrared detectors are used on SAFIRE-A: photoconductive detectors operating at 4 K permit to cover spectral intervals extending from 50 to 250  $\text{cm}^{-1}$ , and bolometric detectors operating at 0.3 K to cover the 10–50  $\text{cm}^{-1}$  region. In this case, a closed circuit  $^3\text{He}$  cooling stage is mounted on the cold plate of the cryostat.

In Fig. 4, two photographs of the instrument are shown. In Fig. 4a most of the EMI shielding enclosing the instrument is removed to show internal parts, in Fig. 4b the instrument is installed on the M-55 Geophysica platform.

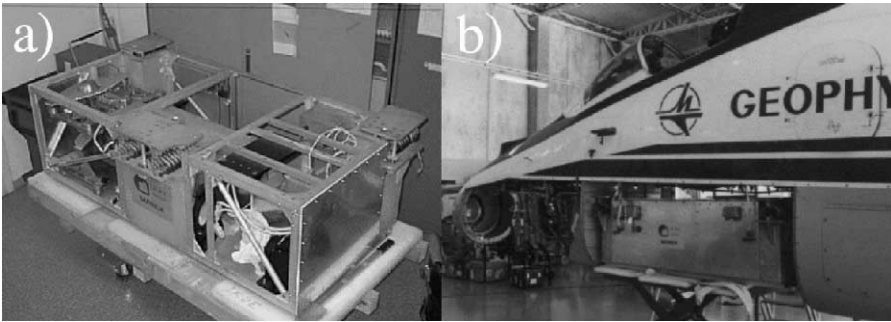


Fig. 4. Photographs of the SAFIRE-A spectrometer: (a) instrument with EMI shielding removed for inspection, (b) instrument ready for integration on the M-55 Geophysica platform.

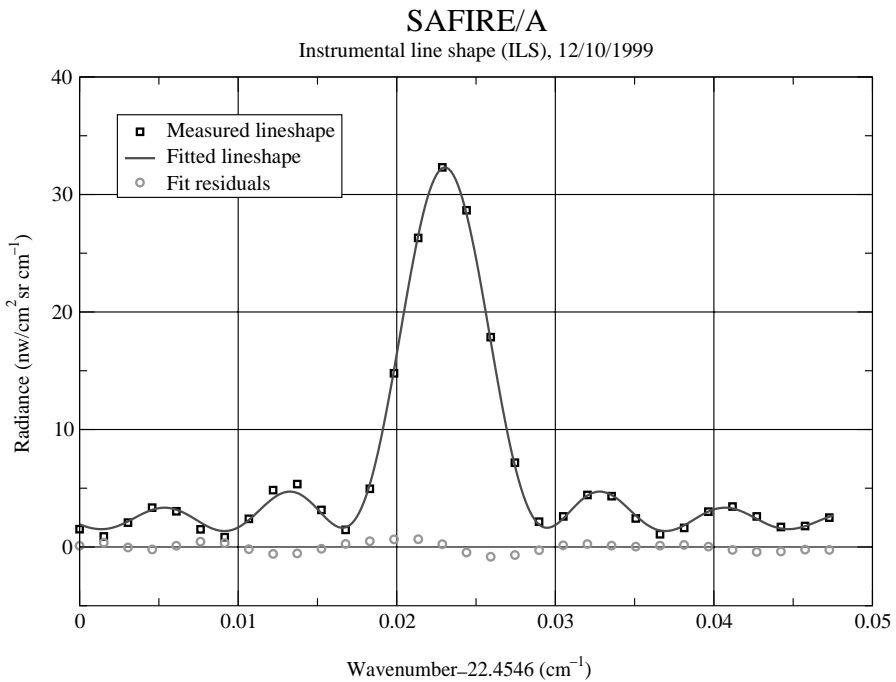


Fig. 5. The instrumental resolution  $\Delta\sigma$  has been measured by fitting the theoretical function for FTS instrumental line shape to a single spectral line. The obtained value is  $\Delta\sigma = 0.004 \text{ cm}^{-1}$ .

## 2.2. Instrument performances

As part of the effort for processing and evaluation of data collected by SAFIRE-A during the APE-GAIA campaign, accurate checks of data quality have been carried out for diagnostics purposes and a new assessment of measured instrument performances has been obtained. Taking into account that important modifications



were recently brought to the spectrometer, with the aim of optimising the instrumental set-up in view of the Antarctic mission, this kind of analysis attained the twofold objective of: verifying the actual improvements in instrument performances, and obtaining a full characterisation of the optimised instrument configuration.

The instrument line shape (ILS) has been determined by averaging multiple spectra recorded with the same acquisition parameters and fitting an isolated spectral line, having a spectral width much lower than instrumental resolution, with the theoretical expression for the FTS lineshape:  $ILS(\sigma) = \sin c(\sigma - \sigma_0)/\Delta\sigma$ .  $\sigma_0$  is the centre frequency of the spectral line and  $\Delta\sigma$  is the spectral resolution. The results are shown in Fig. 5. The obtained value of  $0.004 \text{ cm}^{-1}$  for  $\Delta\sigma$  is in good agreement with the resolution determined by the maximum OPD, showing that the mechanisms limiting the resolution (like field of view effects or instrumental vignetting) have negligible effects.

The frequency calibration stability of SAFIRE-A depends on the reference laser interferometer, that is one of the instrument subsystems that received more significant modifications and improvements. The reference laser stability has been measured by fitting a single line in different spectra selected at regular time intervals during an entire flight (about 6 h of duration). A laser frequency variation  $\Delta v$  will induce a corresponding line centre variation  $\Delta\sigma$  such that  $\Delta v/vL = \Delta\sigma/\sigma_0$ , where  $v_L$  is the laser frequency, and  $\sigma_0$  the centre of the atmospheric spectrum line. In Fig. 6

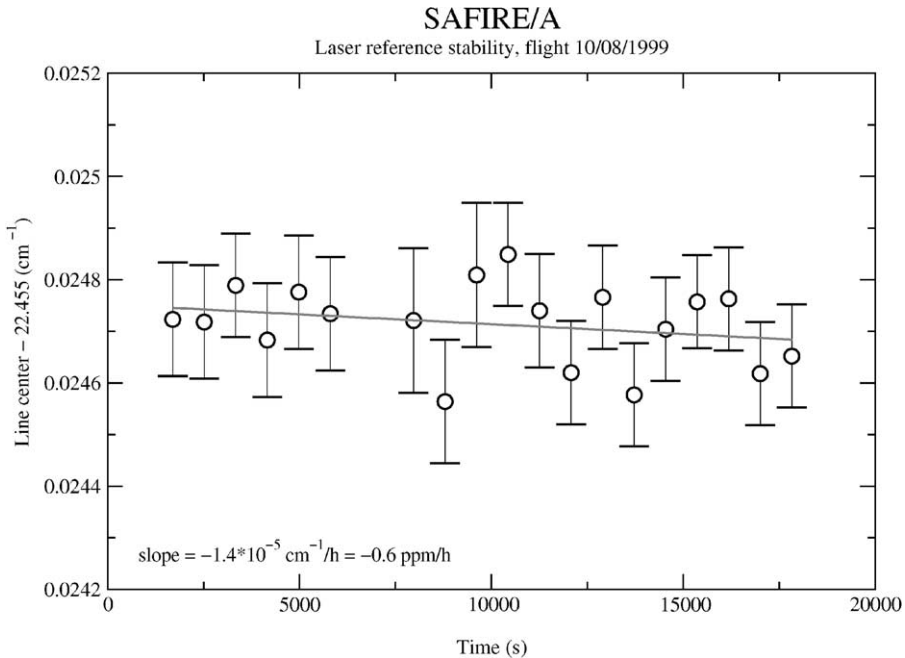


Fig. 6. The reference laser stability can be determined from the variation of the measured value of the centre frequency of an atmospheric line. If we assume that the predominant effect is a slow drift, we obtain a value of  $-0.6 \text{ ppm h}^{-1}$  for the drift ratio.

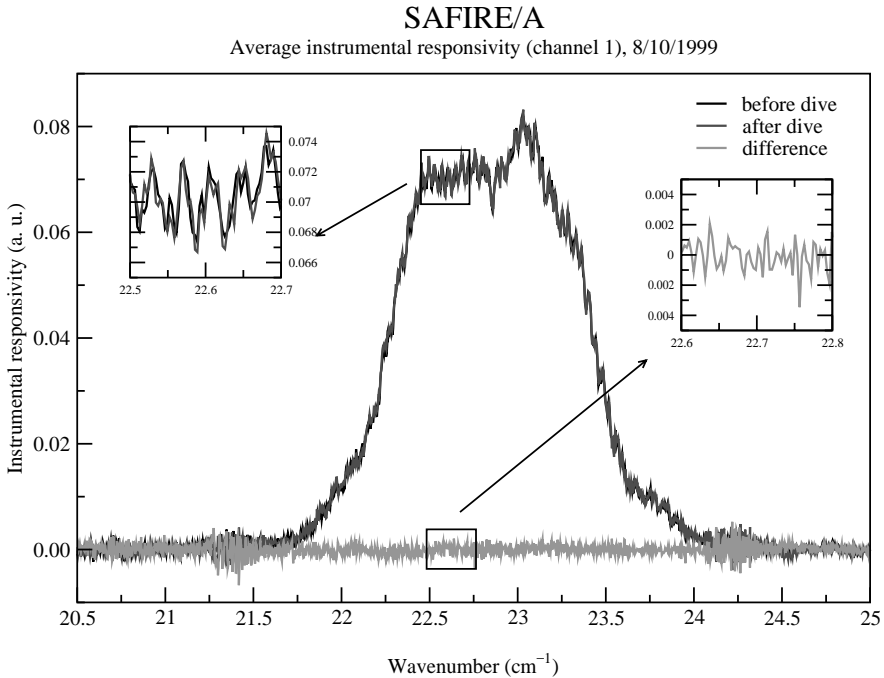


Fig. 7. Responsivity functions obtained from data acquired in the first and second part of the 10/8/1999 flight. The comparison between the two datasets shows that on the time-scale of hours, responsivity variations are below detection noise.

the line centre values are shown. Considering that the expected behaviour is a slow drift due to thermal effects in the laser control electronics, a linear fit is superimposed to the data points. The obtained drift ratio is about  $-0.6 \text{ ppm h}^{-1}$ , well inside instrumental requirements of less than  $6 \text{ ppm h}^{-1}$  [4].

Instrumental responsivity may also vary between two subsequent calibration operations occurring every half an hour. As a consequence, amplitude calibration errors are introduced in the measured spectra. In Fig. 7 two instrumental response functions are shown, measured during the first and the second part of a flight. From this comparison we can determine that responsivity variations on the time-scale of a few hours are below instrumental noise.

### 3. APE-GAIA measurements

The SAFIRE-A spectrometer was flown during the five scientific flights of the APE-GAIA campaign, carried out from the southernmost tip of South America with the aim of studying the chemistry and transport at the boundary of the Antarctic polar vortex. All the scientific flights were performed taking off from the Ushuaia

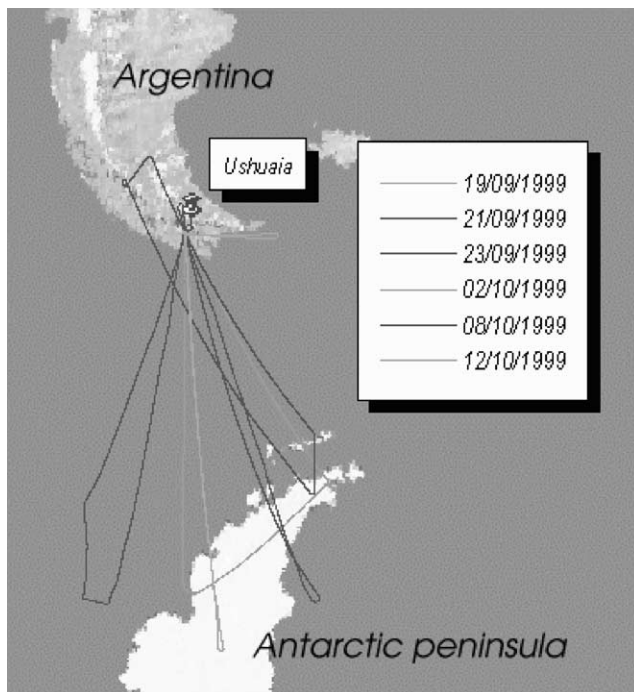


Fig. 8. Map representing the flight paths of the five scientific flights performed by the M-55 Geophysica aircraft during the APE-GAIA campaign.

airport (lat.  $55^{\circ}\text{S}$ , lon.  $68^{\circ}\text{E}$ ) and heading south, towards the Antarctic Peninsula (Fig. 8).

During the campaign the SAFIRE-A spectrometer was equipped with a detector module including a long-wavelength detection channel operating in the  $22\text{--}23.5\text{ cm}^{-1}$  spectral window, and a short-wavelength channel operating at  $123\text{--}125\text{ cm}^{-1}$ . The detected species in the long-wavelength window are  $\text{O}_3$ ,  $\text{ClO}$ ,  $\text{N}_2\text{O}$  and  $\text{HNO}_3$ , the short-wavelength window provides measurements for  $\text{HCl}$  and  $\text{H}_2\text{O}$ .

### 3.1. Observing geometry

During flight, the atmosphere is vertically sampled with limb scanning sequences of ten emission spectra, for a vertical resolution of about  $1.5\text{ km}$ . The acquisition time for a single spectrum is  $30\text{ s}$ , each sequence takes about  $5\text{ min}$ , that, considering the aircraft average ground speed of  $700\text{ km h}^{-1}$  at stratospheric altitude, give an horizontal resolution of about  $50\text{ km}$ , corresponding to  $0.5^{\circ}$  of latitude.

In Fig. 9 a typical limb scanning sequence of atmospheric emission spectra in the  $22\text{--}23.5\text{ cm}^{-1}$  window is shown, where location of spectral features due to the

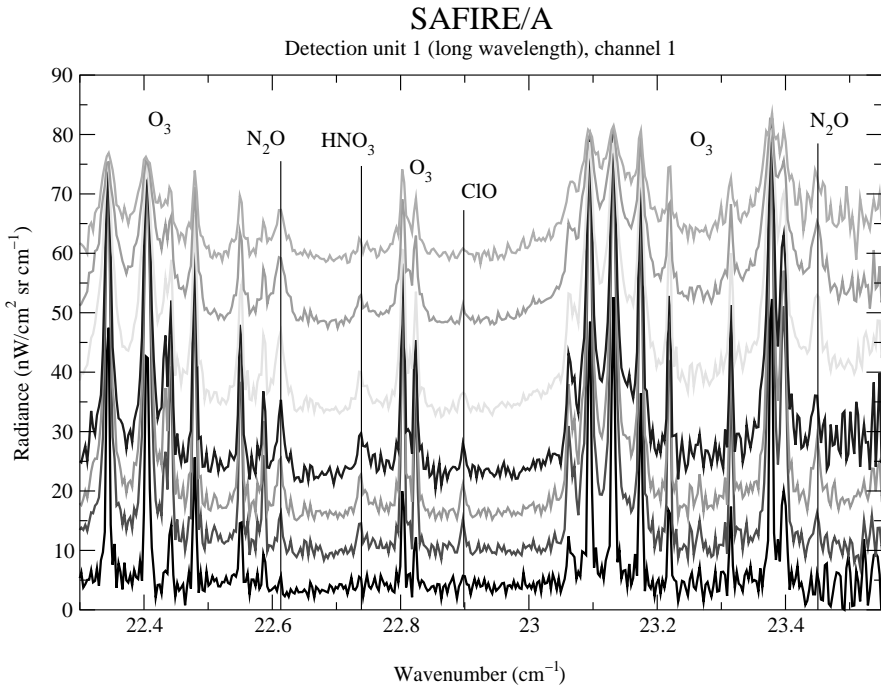


Fig. 9. Limb-scanning sequence of atmospheric emission spectra acquired in the  $22\text{--}23.5\text{ cm}^{-1}$  window. Spectral features due to interesting molecular species are evidenced by vertical lines.

interesting molecular species are evidenced by vertical lines. In Fig. 10 a similar plot is shown for the  $123\text{--}125\text{ cm}^{-1}$  window. In this case only the first few limb scanning angles, corresponding to upper atmospheric layers, are presented. This is due to the greater water vapour contribution to atmospheric opacity, that prevents analysis of lower atmospheric layers. The high frequency channel was affected by very large noise because of the low efficiency at high frequencies of the free standing wire grid beam splitter that was used in order to avoid the acoustic vibrations of the substrate.

### 3.2. Volume mixing ratio measurements

Volume mixing ratio (VMR) vertical profiles of the observed species are retrieved from each limb-scanning sequence by means of a data inversion process [8]. A test and validation of such process is given by the comparison of VMR values at flight altitude obtained from in-situ instruments and corresponding SAFIRE-A retrieved VMR values. Fig. 11 shows the comparison between ozone VMR at flight altitude as measured by the ECOC (Electro-Chemical Ozone Cell) in-situ ozone sonde and SAFIRE-A during the 10/8/1999 scientific flight.

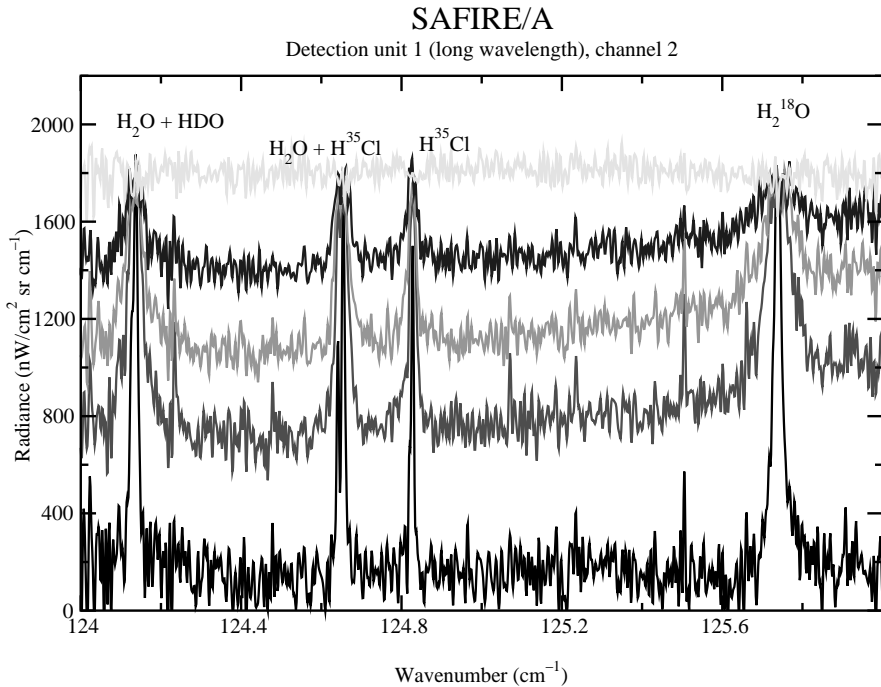


Fig. 10. Limb-scanning sequence of atmospheric emission spectra acquired in the  $124\text{--}126\text{ cm}^{-1}$  window. Spectral features due to interesting molecular species are evidenced by vertical lines. Atmospheric opacity due to water vapour absorption limits analysis to upper atmospheric layers, so only limb scanning angles corresponding to upper layers are presented.

We notice a general agreement between the two data sets plotted in Fig. 11, as well as some occasional differences that are being analysed in order to understand how in-situ and remote sensing instruments may respond to atmospheric gradients.

The most interesting information from SAFIRE-A VMR vertical profiles can be obtained mapping VMR values vs. altitude and aircraft ground position, reconstructing a two-dimensional representation of a slice of atmosphere, thus evidencing geographical variability of stratospheric composition due to chemical and dynamical processes.

In Fig. 12, for instance, VMR maps corresponding to two of the species detected in the long-wavelength channel (ozone and ClO) during the 9/23/1999 flight are shown. In both plots the horizontal axis represents flight time in seconds UTC (Universal Time Co-ordinates). Flight altitude (superimposed to the map) and aircraft latitude (upper graph) are also shown for reference.

The flight considered consists in a first leg in which the aircraft was heading south, crossing the polar vortex edge and entering the vortex, and a second leg heading north, along the same path. Anti-correlation between ozone and ClO evidences the occurrence of chlorine activation and ozone depletion processes as the aircraft approaches the vortex region.

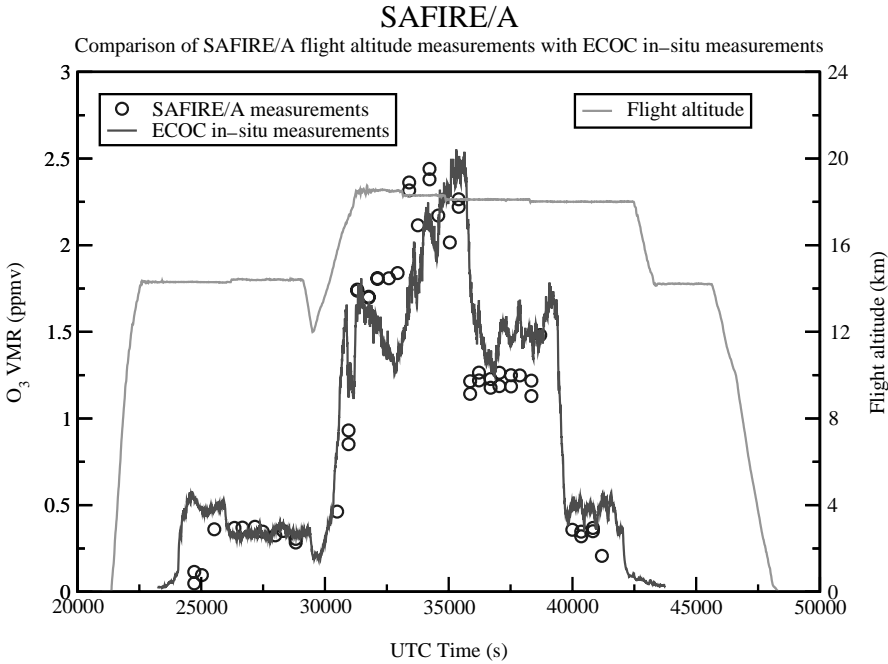


Fig. 11. Comparison between ozone VMR values retrieved at flight altitude from SAFIRE-A data and results obtained from the ECOC in-situ ozone sonde during the 10/8/1999 flight of the APE-GAIA campaign.

#### 4. Conclusions

Emission FTS from airborne platform combines the intrinsic advantages of high sensitivity and selectivity of FTS instruments with the versatility of the aircraft platform, obtaining a multi-purpose tool for the characterisation of upper troposphere/lower stratosphere air masses. Moreover, the limb-sounding observation geometry gives an optimal trade-off between resolution of vertical structures in atmospheric layering and horizontal resolution.

The results obtained by the SAFIRE-A FT spectrometer during the last Antarctic campaign show the capabilities of such a combination of remote-sensing instrument and airborne platform. Two-dimensional mapping of volume mixing ratio of trace species present in concentrations ranging from ppmv to pptv have been obtained in an altitude range extending from 10 to 20 km and along a flight path of a few thousand kilometres. The vertical resolution of such measurements was about 1.5 km and the horizontal resolution about 50 km. These values are adequate to evidence local chemical and dynamical mechanisms, providing the possibility of studying a wide range of atmospheric phenomena, from the seasonal cycle of polar vortex to stratosphere/troposphere exchange or volcanic plumes.

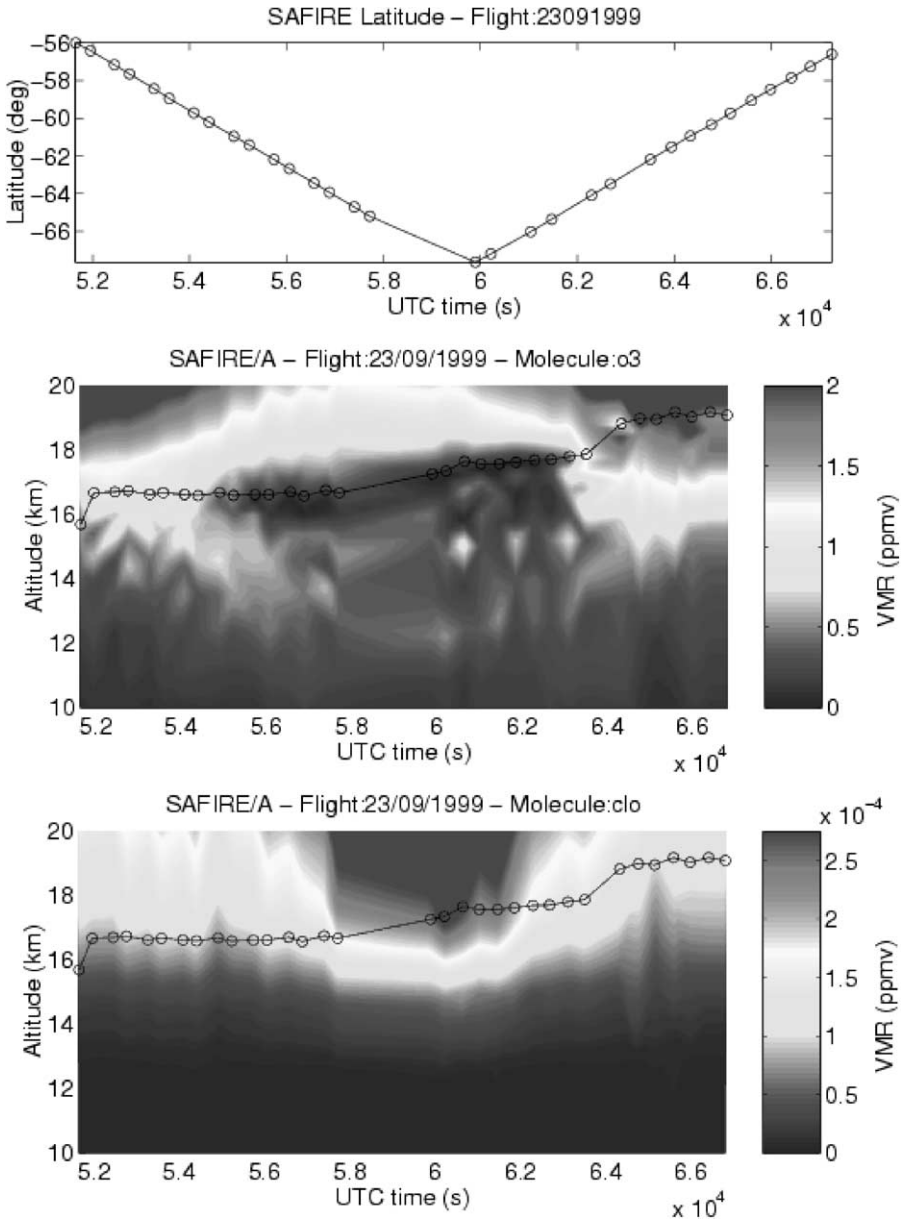


Fig. 12. Ozone and ClO VMR maps obtained from data acquired by SAFIRE-A during the 9/23/1999 scientific flight. Horizontal axis indicates flight time in seconds UTC, VMR units are ppmv. Aircraft flight altitude is superimposed to the map. Aircraft latitude during flight is shown on the upper part of the graph.

## Acknowledgements

This work was supported by the Italian Programme for Research in Antarctica (PNRA-Programma Nazionale di Ricerche in Antartide) and the Italian Space Agency (ASI-Agenzia Spaziale Italiana), which funded most of the activities for the upgrading and utilisation of SAFIRE-A instrument. The authors wish to thank Dr. C. Lee (Queen Mary and Westfield College, London) for providing the operative support on the  $^3\text{He}$ -cooled detector unit. The authors also express their gratitude to Dr. B. Carli (IROE-CNR, Italy) for valuable suggestions and discussions during the course of this research.

## References

- [1] Carli B, Carlotti M. Far-infrared and microwave spectroscopy of the earth's atmosphere. In: Narahari Raom K, Weber A, editors. Spectroscopy of the earth's atmosphere and the interstellar medium. New York: Academic Press, 1992.
- [2] Carli B, Fischer H, Pyle J. Limb sounding techniques for environmental monitoring in the nineties, ESA SP-1140, ESA publication division, ESTEC. The Netherlands: Noordwijk, 1992.
- [3] Chamberlain J. The principles of interferometric spectroscopy. New York: Wiley, 1978.
- [4] Martin DH, Puplett E. Polarised interferometric spectrometry for the millimetre and submillimetre spectrum. *Infrared Phys* 1969;10:105–9.
- [5] Carli B, Ade PAR, Cortesi U, Dickinson P, Epifani M, Gannaway FC, Gignoli A, Keim C, Lee C, Meny C, Leotin J, Mencaraglia F, Murray AG, Nolt IG, Ridolfi M. SAFIRE-A Spectroscopy of the Atmosphere using Far-Infrared Emission/Airborne. *J Atmos Ocean Technol* 1999;16:1313–28.
- [6] Carli B. High-resolution far-infrared FT spectroscopy of the stratosphere: optimization of the optical design of the instrument. *SPIE Proc* 1989;1145:93–989.
- [7] Bianchini G, Lanfranchi M, Cortesi U. Flight qualification of a diode-laser for path difference determination of a high resolution FT spectrometer. *Appl Opt* 2000;39:963–6.
- [8] Ridolfi M, Carli B, Carlotti M, von Clarmann T, Dinelli BM, Dudhia A, Flaud J-M, Höpfner M, Morris PE, Raspollini P, Stiller G, Wells RJ. Optimized forward model and retrieval scheme for MIPAS near-real-time data processing. *Appl Opt* 2000;39:1323–40.